JAERI-M
6598

ON VALIDITY OF THE QUASI-STATIC ASSUMPTION IN TRANSIENT THERMO-HYDRAULIC ANALYSIS OF GCFR

June 1976

Hiroshi KAWAMURA

日本原子力研究所
Japan Atomic Energy Research Institute

この報告書は，日本原子力研究所がJAERI-Mレポートとして，不定期に刊行している研究報告書です．入手，複製などのお問合わせは，日本原子力研究所技術情報部（茨城県那珂郡東海村）あて，お申しこしください．

JAERI-M reports, issued irregularly, describe the results of research works carried out in JAERI. Inquiries about the availability of reports and their reproduction should be addressed to Division of Technical Information, Japan Atomic Energy Research Institute, Tokai-mura, Naka-gun, Ibaraki-ken, Japan.

JAERI-M 6598

Validity of the Quasi-Static Assumption in Transient Thermo-Hydraulic Analysis of GCFR

Hiroshi KAWAMURA

Division of Reactor Engineering, Tokai, JAERI

(Received June 2, 1976)

In reactor transient analysis, the friction factor and the heat transfer coefficient are assumed to be equal to the steady-state ones. Validity of this 'quasi-static assumption' is examined.

The transient turbulent heat transfer in a circular tube is examined numerically and experimentally in step change of the pressure gradient or the heat input. Transient variations of the friction factor and the heat transfer coefficient are obtained. The times required for the flow velocity and the heat transfer coefficient to attain the steady-state values are studied.

The steady state friction factor and the heat transfer coefficient are found to be applicable in transient analyses of GCFR.

JAERI-M 6598

GCFRの過渡熱流力解析における準定常仮定の妥当性について

日本原子力研究所・東海研究所・原子炉工学部

河村　洋

（1976年6月2日受理）

GCFR（ガス冷却高速炉）をはじめとする原子炉の安全解析においては，管摩擦係数や熱伝達率の値は，非定常状態においても定常値に等しいと仮定される。本報では，この準定常仮定の妥当性を検討した。

流れの圧力頭あるいは燃料内の発熱が時間的にステップ状に変化する場合について，円管内乱流の非定常熱伝達を数値的および実験的に研究した。管摩擦係数および熱伝達率の時間変化を求め，流速や熱伝達率が新しい定常値に達するに要する時間を検討した。

以上の結果，GCFRの過渡状態の解析にあたっては，管摩擦係数や熱伝達率の定常値が近似的に適用できることがわかった。

目　次　な　し

I. INTRODUCTION

The momentum equation and the energy equation for a coolant flow must be solved in a reactor transient analysis. The friction factor f and the heat transfer coefficient α are introduced into these equations. The friction factor is defined as

$$f = \tau / (\tfrac{1}{2} \rho_f \bar{u}^2), \tag{1}$$

and the heat transfer coefficient is

$$\alpha = q_n / (T_w - \bar{T}_f). \tag{2}$$

By introducing f and α, one need not solve transient profiles of velocity and temperature in the coolant. Because the transient values of f and α are not known, they are assumed equal to the steady state values.

The momentum equation solved in reactor transient analysis is

$$\frac{\partial \bar{u}}{\partial t} = \frac{g_c}{\rho_f} \cdot \left| \frac{\partial P}{\partial x} \right| - f_{st} \frac{\bar{u}^2}{D/2}, \tag{3}$$

and the energy equation is

$$\frac{\partial \bar{T}_f}{\partial t} + \bar{u} \frac{\partial \bar{T}_f}{\partial x} = \alpha_{st} \frac{4}{D(\rho c_p)_f} \cdot (T_w - \bar{T}_f), \tag{4}$$

where f_{st} and α_{st} are the friction factor and the heat transfer coefficient in the steady state, respectively. These equations are called the quasi-static equations. The quasi-static assumption is made in almost all the transient analysis codes, but has not been examined well. The purpose of the present study is to examine validity of the quasi-static assumption by analyzing the transient turbulent hydraulics and heat transfer.

Many works have been made on the transient laminar heat transfer, but relatively few works on the transient turbulent heat transfer. Sparrow-Siegel[1] solved the transient energy

equation for stepwise time variation of the wall temperature. Soliman[2] studied the transient heat transfer from a plate of a finite heat capacity to a developing flow of water. Gopalakrishnan, et al.,[3] solved the transient energy equation numerically and obtained variation of the heat transfer coefficient when the power increased exponentially with a constant flow. The present author[4] analyzed the transient turbulent heat transfer in an annulus. The flow was steady and the heat input was increased stepwise. The conditions for the quasi-static assumption were studied. He[5] also studied flow transient, where the heat input was constant and the flow velocity was varied with time.

In the present paper, the studies on power and flow transients are summarized. The transient two-dimensional momentum and energy equations are solved for step changes of the power input and the pressure gradient. These solutions are compared with those of the quasi-static equations and validity of the quasi-static assumption is examined.

II. NUMERICAL ANALYSIS

II.A Assumptions

1) A very long circular tube is assumed, so the flow is fully developed. 2) The heating wall has a finite thermal capacity, but the temperature distribution inside the wall is neglected. 3) The tube wall is insulated on the outside. 4) Properties are independent of the temperature, and the flow is incompressible.

II.B Two-dimensional equations

A co-ordinate system is shown in Fig. 1. The wall is heated in $x \geq 0$. The momentum equation is

$$\frac{\partial u}{\partial t} = \frac{g_c}{\rho_f} \cdot \left|\frac{\partial P}{\partial x}\right| + \frac{1}{r}\frac{\partial}{\partial r}\left[(\varepsilon_M + \nu)\, r \frac{\partial u}{\partial r}\right]. \qquad (5)$$

The energy equation is

$$\frac{\partial T_f}{\partial t} + u \frac{\partial T_f}{\partial x} = \frac{1}{r} \frac{\partial}{\partial r} \left[(\varepsilon_H + a_f) r \frac{\partial T_f}{\partial r} \right]. \quad (6)$$

These two equations contain two co-ordinates x and r; but Eq. (5) is one-dimensional because u does not vary in the direction of x. However, Eq. (5) will also be called two-dimensional for convenience. The correlations for ε_H and ε_M are described later.

The boundary conditions are u = 0, T = T_w, and $\partial T/\partial r = -q_n/\lambda_f$ at r = D/2. Heat balance in the wall is

$$q_n(t) = q_G(t) - H \frac{\partial}{\partial t} T_w \quad (7)$$

where q_G is the heat generation rate in the wall. Other conditions are $\partial u/\partial r = 0$ and $\partial T/\partial r = 0$ at r = 0, and T = 0 at x = 0.

II.C Quasi-static calculation

The quasi-static equations, Eqs. (3) and (4), are solved with the assumption that f_{st} and α_{st} are constant with time. The steady state friction factor f_{st} and heat transfer coefficient α_{st} are obtained by the numerical calculations of Eqs. (5) and (6).

III. POWER TRANSIENT

The transient heat transfer for a step increase of power input is studied experimentally and analytically in this chapter. The flow velocity is assumed constant with time.

III.A Numerical analysis

The two dimensional equations, Eqs. (5) and (6), are solved numerically together with Eq. (7) for a stepwise increase of power input. The heat input in Eq. (7) is given as

$$q_G = \begin{cases} q_{G,0} & t \leq 0 \\ q_{G,1} & t > 0, \end{cases} \tag{8}$$

where $q_{G,0}$ is the initial heat input and either zero or not zero. As the flow is assumed steady, $\partial u/\partial t$ in Eq. (3) is set equal to zero in this chapter.

The momentum eddy diffusivity used is the Reichardt's[6] correlation multiplied by the damping factor postulated by Wilson-Medwell.[7]

$$\frac{\varepsilon_M}{\nu} = 0.4 \frac{r_w u^*}{3\nu}\left[\frac{1}{2} + \left(\frac{r}{r_w}\right)^2\right]\cdot\left[1 - \left(\frac{r}{r_w}\right)^2\right]\cdot\left[1 - \exp(-y^+/A^+)\right]. \tag{9}$$

The damping constant A^+ is so decided that the steady state heat transfer coefficient obtained numerically coincides with that obtained experimentally. The value of A^+ is found about 40 for $Re \geq 10^4$ and larger for $Re < 10^4$.

The eddy diffusiviry ratio $\sigma = \varepsilon_H/\varepsilon_M$ is given referring to Mizushina[8] as follows:

$$\sigma = 1.5\phi\left[1 - \exp(-1/\phi)\right] \tag{10}$$

$$\phi = (\varepsilon_M/\nu) Pr / \left[4.13 + 0.743 (\varepsilon_M/\nu)^{1/2} Pr^{1/3}\right]. \tag{11}$$

III.B Experiment

Figure 2 shows the experimental apparatus. The test section was a stainless steel tube installed horizontally. Two tubes were tested. They had different diameters and wall thicknesses as shown in Fig. 2. Both tubes were 2 m long. A heated section was 30 D located near the exist of the test section. It was heated by electric current. The 23 D of the heated section was devoted to a thermally developing section. A temperature measuring section was 5 D located in the immediate down-stream of the thermally developing section.

The upstream of the heated section acted as a hydrodynamically developing region. Its length was 32 D in the test

section A and 77 D in B.

The mean temperature in the measuring section $\overline{T}_w$ was obtained from an increment of the electric resistance of the tube wall. A resistance double bridge was devised to measure the increment of the tube wall resistance. The temperature coefficient of the resistance was measured prior to the experiment.

Heat generation rate per unit heat transfer area q_G was obtained from the electric current and voltage drop across the measuring section. The net heat flux from the tube wall to the fluid q_n was calculated from the heat balance relation, Eq. (7).

Some results of the transient experiments are shown in Fig. 3. Two examples for different Reynolds numbers are compared in the figure. The heat transfer coefficient decreases with time and reaches the steady state value asymptotically. The time required for the heat transfer coefficient to reach the steady state becomes small when the Reynolds number is large.

The solid lines in Fig. 3 show the numerical solutions. They agree well with the experimental results.

The quasi-static solution is the solution with the quasi-static assumption described in II.C. The difference between the quasi-static solution and the experimental result increases with decreasing Reynolds number.

The conduction solution in Fig. 3 is a numerical solution of the equation

$$\frac{\partial T_f}{\partial t} = \frac{1}{r}\frac{\partial}{\partial r}\left[(\varepsilon_H + q_f)\, r \frac{\partial T_f}{\partial r}\right]. \tag{12}$$

This is derived from Eq. (5) by neglecting the convection term $u(\partial T_f/\partial x)$. Equation (12) has the same form as the thermal conduction equation; so, its solution is called the conduction solution in the present paper.

The heat transfer coefficient by the conduction solution agrees well with the experimental one except at large times. The reason why the convection term can be neglected at small times was discussed in Ref. (4). Briefly, it is because $\partial T_f/\partial x$ remains zero at small times if the heat input is

initially zero and axially uniform.

III.C Simplified analytical solution

An approximate solution for the transient variation of the heat transfer coefficient was derived in Ref. (4), by solving the conduction equation Eq. (12) with the approximation:

$$\varepsilon_H + q_f = q_f (by+1)^n \tag{13}$$

where b is a constant dependent on fluid properties and Reynolds number. If n in Eq. (13) is assumed 2, Eq. (12) could be solved[4] analytically.

Two non-dimensional parameters relevant to the transient heat transfer were derived from the approximate equation. The first is a non-dimensional time Z_p defined as

$$Z_p = \frac{\alpha_{st}^2}{4(\lambda\rho c_p)_f} t \,. \tag{14}$$

The second parameter is

$$\beta_p = \frac{\alpha_{st} H}{(\lambda\rho c_p)_f} \,, \tag{15}$$

where H is the wall heat capacity per a heat transfer area, expressed as

$$H = d_w^* (\rho c_p)_w, \tag{16}$$

where d_w^* is the equivalent wall thickness defined as

$$d_w^* = d_w(1 + d_w/D) \tag{17}$$

The variation of the heat transfer coefficient obtained by the experiment is plotted versus the real time in sec for $q_{G,0} = 0$ in Fig. 4(a). The variation depends on the Reynolds number, the tube diameter and wall thickness. The same data are re-plotted against the non-dimensional time Z_p in Fig. 4(b). The variation of the heat transfer coefficient is well correlated

by Z_p and slightly depends on β_p. It is thus indicated that the non-dimensional time Z_p is a critical parameter relating with the variation of heat trnasfer coefficient.

One can see in Fig. 4(b) that the heat transfer coefficient reaches the steady state roughly when $Z_p \sim 1$. The time required is slightly dependent on β_p. Since the heat transfer coefficient approaches to the steady state asymptotically, it is often sufficient to know only the order of magnitude of the steady state time. For such the purpose, the time required for heat transfer coefficient to reach the steady state may be given as $Z_p \sim 1$ or

$$t_{st,\alpha} \sim 4(\lambda\rho c_p)_f / \alpha_{st}^2 \tag{18}$$

The parameters Z_p and β_p are rewitten as

$$Z_p = \alpha_f t/(4\ d_f^{*2}) \tag{19}$$

$$\beta_p = \frac{d_w^*(\rho\ c_p)_w}{d_f^*(\rho\ c_p)_f}\ , \tag{20}$$

where d_f^* is λ_f/α_{st} and has the dimension of length.

If the fluid is assumed as a semi-infinite solid with a uniform thermal conductivity λ_f, d_f^* is the thickness of the temperature-varying layer which gives the heat transfer coefficient of α_{st} in the steady state (see Fig. 6). Thus, Z_p is interpreted as the Fourier Number where the characteristic length is the equivalent thermal boundary layer thickness d_f^*. The time for the temperature variation to develop in the equivalent thermal boundary layer is an order of $Z_p \sim 1$, and it is roughly equal to the steady-state time of the heat transfer coefficient for a stepwise heat input.

Equation (20) shows that β_p is the ratio of the heat capatity of the wall to that of the equivalent thermal boundary layer. When $\beta_p >> 1$, most of the heat generated is stored in the wall; when $\beta_p < 1$, more heat is transferred to the fluid

than that stored in the wall. So, the transient effect in the heat transfer is prominent when $\beta_p < 1$.

To examine the validity of the quasi-static assumption, the ratio of the wall temperature with the quasi-static assumption to the one without the assumption is shown in Fig. 5 for various β_p's with the approximation of Eq. (13). The ratio becomes much less than unity if $\beta_p << 1$, while it approaches unity for all times with increase of β_p. Thus, the quasi-static approximation is valid roughly when $\beta_p \geq 10$.

III.D Effect of initial power input

Figure 7 shows the results by experiment for three different initial heat inputs. When $q_{G,0} \neq 0$, a maximam appears in the variation of the heat transfer coefficient. The maximum decreases and the transient effect becomes less prominent with increases of $q_{G,0}$.

The maximum in heat transfer coefficient is already found analytically in Ref. (4). If $q_{G,0} = 0$, the temperature in fluid is uniform at $t = 0$; so, the heat transfer coefficient at small times is determined by the transient heat conduction in the fluid. The heat transfer coefficient becomes infinite at the beginning of the transient. When $q_{G,0} \neq 0$, a steady state temperature distribution already exists at $t = 0$. The heat transfer coefficient is determined by the steady state temperature distribution; thus $\alpha = \alpha_{st}$ at $t \to 0$.

III.E Application to reactors

Values of β_p and $t_{st,\alpha}$ are calculated for several types of power reactors, and listed in Table I. The numbers give only the order of magnitude. The time required for the heat transfer coefficient to reach the steady state $t_{st,\alpha}$ is very short in GCFR and relatively long in PWR. The analysis in Section III.C showed that the quasi-static assumption is valid if $\beta_p > 10$. TABLE I indicates that the quasi-static assumption brings some error for LMFBR but it is not so large.

If the power transient occurs at a lower Reynolds number, β_p is smaller and the transient effect is more prominent. At the normal operational condition of PWR, the quasi-static assumption is valid, while some error is introduced by the assumption at Reynolds numbers less than 10^4.

In GCFR, β_p is so large that the quasi-static assumption is valid at least if the flow is turbulent. This is because the heat capacity of fuel is much larger than that of coolant in GCFR.

IV. FLOW TRANSIENT

IV.A Analysis

The two dimensional equations, Eqs. (5) and (6) are solved numerically for a step change of pressure gradient. The pressure gradiant in Eq. (5) is given as

$$\left|\frac{\partial P}{\partial x}\right| = \begin{cases} P_{x,0} & t \leq 0 \\ P_{x,1} & t > 0 \end{cases} \tag{21}$$

The heat generation rate q_G in Eq. (7) is constant with time.

The momentum eddy diffusivity is calculated by the Prandtl's mixing length model.

$$\varepsilon_M = \ell^2 \left|\frac{\partial u}{\partial r}\right| . \tag{22}$$

Here ℓ is the Prandtl's mixing length given as

$$\ell = \begin{cases} C_\ell D & y \geq (C_\ell/\kappa_\ell)D \\ \kappa_\ell y, & y < (C_\ell/\kappa_\ell)D \end{cases} \tag{23}$$

where $C_\ell = 0.045$ and $\kappa_\ell = 0.4$ in the present calculation.

Very close to the wall, ℓ is damped as postulated by van Driest[9]:

$$\ell = \kappa_\ell y \left[1 - \exp(-y^+/A^+)\right]. \tag{24}$$

The damping constant A^+ is about 20 - 30 depending on the Reynolds number.

The thermal eddy diffusivity ε_H is calculated by Eqs. (10) and (11).

The present method is proved successful in calculation of the steady state turbulent flow. The method is here assumed applicable for the transient flow. Although the steady state mixing theory is used for ε_M, the value of ε_M is not equal to its steady state value. The momenturm equation Eq. (5) gives a transient velocity profile, and then Eq. (22) gives a transient ε_M.

IV.B Transient hydraulics

Figure 8 gives an example of the transient numerical calculation. The pressure gradient increases stepwise at t = 0. The flow is accelerated from Re = 10^4 to 10^5. The suffix 1 represents the final steady state, while st shows the steady state value for instantaneous Reynolds number.

The velocity reaches a new steady state at about 1 sec in this example. The time as an abscissa is given for water in a tube of D = 2 cm. The other abscissa Z_u is a non-dimensional time defined by

$$Z_u = 4(f_1/D)\bar{u} \cdot t. \tag{25}$$

It is found[5] that the mean velocity reaches the new steady state at Z_u = 3-4, or

$$t_{st,\bar{u}} \sim D/(f_1 \cdot \bar{u}_1). \tag{26}$$

The friction factor becomes much larger than the quasi-static value in the case of acceleration. The friction factor ratio f/f_{st} increases temporarily, then decreases asymptotically down to 1. The peak value is about 1.7 in this example. In very severe transient from Re = 10^4 to 10^6, the ratio f/f_{st} becomes as high as 7.

Figure 9 illustrates the case of deceleration from Re = 10^5 to 10^4. The flow reaches a new steady state at about 4 sec. The friction factor ratio f/f_{st} is slightly less than 1.

The friction factor is nearly the same as the quasi-static value in the deceleration.

In the deceleration, f/f_{st} does not differ much from unity. Even in the case of the severe transient of Re = 10^6 to 10^4, the ratio is only slightly less than unity.

The present interest is in validity of the quasi-static equation rather than in variation of the friction factor. The solution of the quasi-static momentum equation $\bar{u}_{quasi}$ is compared with the mean velocity $\bar{u}$ obtained from the two-dimensional momentum equation in Fig. 10. The ratio $\bar{u}_{quasi}/\bar{u}$ is very close to unity in the acceleration; it deviates about 5 - 10 % from unity in the deceleration.

In the accelerated flow, the friction factor deviates considerably from its steady state value; nevertheless, the velocity variation is nearly quasi-static. This can be explained by comparing the two terms on the right hand side of Eq. (3). These two terms have the same values at the initial state, then the pressure gradient increases compared with the friction. So, the friction factor has small effect on the velocity variation even when it changes much. In other words, inertia of the fluid is dominant and the friction is neglible at the initial stage of the transient. With lapse of time, the friction term becomes again important. At this time, however, the friction factor has already reached to its new steady state value. This is the reason why the quasi-static momentum equation is valid for the accelerated flow.

In the case of deceleration, the friction term is dominant. Only slight error in the friction factor results in a relatively large error in velocity calculation. However, since the friction factor does not deviate from the steady state value in the decelerated flow, the error in velocity calculation is less than 10 % even in the severest transient of Re = 10^6 to 10^4.

In conclusion, the quasi-static momentum equation is roughly valid for both the acceleration and the deceleration. The error due to the quasi-static assumption is small for the accelerated flow, and relatively large, but less than 10 %, for

the decelerated flow.

IV.C Transient heat transfer

Figure 11 shows variation of α/α_{st} for various initial and final Reynolds numbers. In the accelerated flow, the heat transfer coefficient ratio α/α_{st} decreases well below unity, and it depends much on the initial and final Reynolds numbers. In the decelerated flow, α/α_{st} is a little larger than unity, and it does not depend so much on the initial and final Reynolds numbers.

An error in the wall temperature difference $\Delta T_w = T_w - \bar{T}_f$ due to the quasi-static assumption is shown in Fig. 12 for the deceleration. Here, $\Delta T_{w,quasi}$ is obtained from the quasi-static equations (3) and (4), while ΔT_w from the two-dimensional equations (5) and (6). The parameter β_u is a non-dimensional number pertinent to the wall heat capacity. It is defined as

$$\beta_u = 4 f_1 Re_1 Pr \tilde{H}/Nu_1 \tag{27}$$

This parameter has been derived intuitively rather than mathematically. It is propotional to the heat capacity ratio

$$\tilde{H} = d_w^* (\rho C_p)_w / [D \cdot (\rho C_p)_f] \tag{28}$$

The physical significance of β_u is

$$\beta_u \propto \frac{\text{Time for } \Delta T_w \text{ to reach steady state (in case of a large wall heat capacity)}}{\text{Time for } \bar{u} \text{ to reach steady state}} \tag{29}$$

Fig. 12 shows that α/α_{st} is slightly dependent on the wall heat capacity, and $\Delta T_{w,quasi}/\Delta T_w$ is more dependent. The error in the quasi-static ΔT_w is due to the combined effect of both errors in $\bar{u}$ and α. When the wall heat capacity β_u becomes large, the error in $\Delta T_{w,quasi}$ becomes small. The error is 18 % at most.

So, the quasi-static energy equation is thus approximately valid in the case of deceleration. Moreover, the quasi-static assumption results in a slightly higher wall temperature than the actual one. This error is usually on the safe side in reactor accident analyses. These points are important because the flow deceleration is to be solved in almost all reactor safety analyses.

Figure 13 illustrates the effects of wall heat capacity β_u and Prandtl number Pr on variation of α/α_{st} in the accelerated flow. The variation of α/α_{st} does not much depend on Pr if $\beta_u > 0$. Especially, the values of α/α_{st} at the plateau are nearly equal to different Pr, when β_u is constant and $\beta_u >> 0$.

The wall temperature obtained from the quasi-static equation is compared with that obtained from the two-dimensional equation in Fig. 14. The ordinate is the ratio $\Delta T_{w,quasi}/\Delta T_w$. When $\beta_u > 1$, the ratio is almost unity regardless of Pr. Figure 14 is an example of the severe acceleration from Re = 10^4 to 10^6. In less severe accelerations, the ratio is closer to unity.

The variation of mean fluid temperature was also examined. It is approximately quasi-static when $\beta_u > 1$. So, the quasi-static energy equation is thus valid also in the acceleration if $\beta_u > 1$.

IV.D Application to reactors

Table II gives the time for the flow to reach a new steady state $t_{st,\bar{u}}$, the heat capacity ratio H, and the non-dimensional heat capacity β_u. In the wall heat capacity included are the heat capacities of a fuel and a clad. The values are not accurate but give the order of magnitude.

The time required for the flow to reach a new steady state is very short in GCFR and relatively long in PWR. The time in LMFBR is intermediate between these two. In GCFR, the flow can follow a change of the pressure gradient rapidly. In PWR, a rather large time delay should be expected.

The heat capacity ratio H and the non-dimensional heat

capacity β_u are large in GCFR. So, the quasi-static energy equation is valid for both accelerated and decelerated flows. The reason for $\tilde{H}$ and β_u to be so large in GCFR is that ρc_p of the fuel is much larger than that of the coolant. So, it can be expected that the quasi-static energy equation is valid for all types of gas cooled reactors.

The non-dimensional heat capacity β_u is nearly in PWR and slightly less than 1 in LMFBR. The quasi-static assumption is approximately valid for deceleration, but these β_u's are rather delicate for acceleration. From the present results, it is expected that the quasi-static assumption will not cause serious error in PWR and LMFBR, too.

V. CONCLUSION AND FURTHER STUDIES

The steady state friction factor and heat transfer coefficient are approximately applicable to the transient analysis of GCFR, if the flow is in the turbulent region.

Further studies are required for some effects neglected in the present study, such as thermal resistance in fuel, variation of physical properties, effects of cladding and roughness. The thermal resistance in fuel and cladding will reduce the transient effect in heat transfer, while the property variation will make it more prominent.

It has been pointed out that only a slight error in friction factor brings a fairly large error in flow velocity calculated for the flow deceleration. The transient friction factor has been found nearly equal to the steady state value in the turbulent region. So, the steady state correlation is appricable to the transient state of the turbulent flow. In the transition region, however, even the steady state correlation has not been established well.

The flow decelerations are calculated with three friction correlations in the transition region. They are compared in

Fig. 15. The correlation I is an experimental result by Patel & Head[10] for a circular tube. The correlation II is the one assumed often for convenience. The correlation III is typical in rod bundles. (see Reheme[11], for example.) The calculated velocities are given in term of the Reynolds number. The flow is decelerated from Re = 10,000 to 500. Large differences exist between the velocities calculated with different friction correlations.

The flow in the transition region has a 'transient' nature even in the steady state, because the flow alternates in time between being laminar or turbulent. It is uncertain whether the transient friction factor for the flow deceleration is nearly equal to the steady state value in the transition region or not. There is an uncertainty in the transient heat transfer coefficient, too. Studies are thus required for the transient friction factor and heat transfer coefficient in the transition region.

Acknowledgement

A part of the present work (Chapter IV) was made in Kernforschungszentrum Karlsruhe in F.R. Germany. The author would like to express his gratitude to Prof. Dr. K. Wirtz, Dr. M. Dalle Donne and Dr. D. Wilhelm for their helps and discussions.

Nomenclature

a	:	thermal diffusivity, m^2/sec
c_p	:	specific heat capacity, $kcal/kg_m$ deg
D	:	diameter of a tube, m
d_w	:	thickness of a heating wall, m
f	:	friction factor
g_c	:	standard acceleration, $kg_m/kg_f.m/sec^2$
Nu	:	Nusselt number = $\alpha D/\lambda_f$
H	:	wall heat capacity per unit heat transfer surface, $kcal/m^2$ deg
$\tilde{H}$	:	heat capacity ratio, Eq. (28)

ℓ	:	mixing length, m
P	:	pressure, kg_f/m^2
Pr	:	Prandtl number = ν_f/a_f
q_G	:	heat generation rate per unit heat transfer surface, $kcal/m^2$ sec
q_n	:	net heat flux to fluid, $kcal/m^2$ sec
Re	:	Reynolds number = $\bar{u}D/\nu_f$
r	:	radius, m
T	:	temperature, deg, °C
$\bar{T}_f$	:	mixed mean temperature of fluid, deg, °C
ΔT_w	:	= $T_w - \bar{T}_f$
t	:	time, sec
u	:	velocity, m/sec
$\bar{u}$	:	mean velocity, m/sec
u*	:	friction velocity = $\sqrt{g_c \cdot \tau/\rho_f}$, m/sec
x	:	axial distance, m
y	:	distance from a wall, m
y^+	:	= yu^*/ν_f
Z_p	:	non-dimensional time for power transient, Eq. (14)
Z_u	:	non-dimensional time for flow transient, Eq. (25)

Greek

α	:	heat transfer coefficient $kcal/m^2$ sec deg
β_p	:	non-dimensional wall heat capacity for power transient, Eq. (15)
β_u	:	non-dimensional wall heat capacity for flow transient, Eq. (27)
ε_H	:	thermal eddy diffusivity, m^2/sec
ε_M	:	momentum eddy diffusivity, m^2/sec
λ	:	thermal conductivety, kcal/m sec deg
ν	:	kinematic viscosity of fluid, m^2/sec
ρ	:	density, kg_m/m^3
τ	:	wall shear stress, kg_f/m^2

Subscripts

f :	fluid
p :	power transient
quasi:	quasi-static solution
in :	inlet
st :	steady state
u :	flow transient
tran.:	transient solution without quasi-static assumption
w :	heat transfer wall surface
0 :	initial state
1 :	final state

References

(1) Sparrow, E.M. and Siegel, R., Trans. ASME, Ser. C, 82 – 3, (1960), p. 170.
(2) Soliman, M., SAN-1011 (1966).
(3) Gopalakrishnan, A., V.E. Schrock, & J.E. Meyer, ASME Paper 72-WA/HT-50, (1972).
(4) Kawamura, H., Heat Transfer – Japanese Research, 3 – 1, (1974), p. 45.
(5) Kawamura, H., KFK – 2166, (1975).
(6) Rechardt, H., Z. AMM., 31, (1951), p. 208.
(7) Wilson, N.W. & Medwell, J.O., J. Heat Transfer, 93C, (1971), p. 25.
(8) Mizushina, T., Jour. Japan Soc. Mech. Engirs., 72, (1969), p. 328, (in Japanese).
(9) Van Driest, E.R., J. Aeron. Sci., 23, (1956), p. 1007.
(10) Patel, V.C. & Head, M.R., J. Fluid Mech., 38, (1969), p. 181.
(11) Rehme, K., Forsch. Ing. – Wes., 35, (1969), p. 107
(12) Simon, R.H., J.B. Dee, & W.I. Morita, CONF – 740501, Paper 5 – 3, (1974).
(13) Directory of Nuclear Reactors, Vol. IV, (1962), IAEA.
(14) Design Studies of a 1000 – MWe Fast Reactor, Power Reactor Technology, 8 – 2, (1964/65), p. 147.

TABLE I Parameters for power transient

		Eq.	GCFR[a]		PWR[b]		LMFBR[c]	
Reynold number	Re		10^4	10^5	10^4	10^5	10^4	10^5
Steady state time for heat transfer coefficient	$t_{st,\alpha}$ (msec)	(18)	28	.68	1400	34	91	45
Non-dimensional heat capacity	β_p	(15)	720	4600	7.0	45	3.8	5.3

TABLE II Parameters for flow transient

		Eq.	GCFR[a]		PWR[b]		LMFBR[c]	
Final Reynold number	Re_1		10^4	10^5	10^4	10^5	10^4	10^5
Steady state time for flow	$t_{st,u}$ (sec)	(26)	.14	.023	7.0	1.2	1.8	.31
Heat capacity ratio	$\tilde{H}$	(28)	23		0.19		0.712	
Non-dimensional heat capacity	β_u	(27)	152	143	1.6	1.5	.20	.85

a GA 300 MWe demonstration plant (12)

b Indian Point (13)

c GE 1000 MWe design study (14)

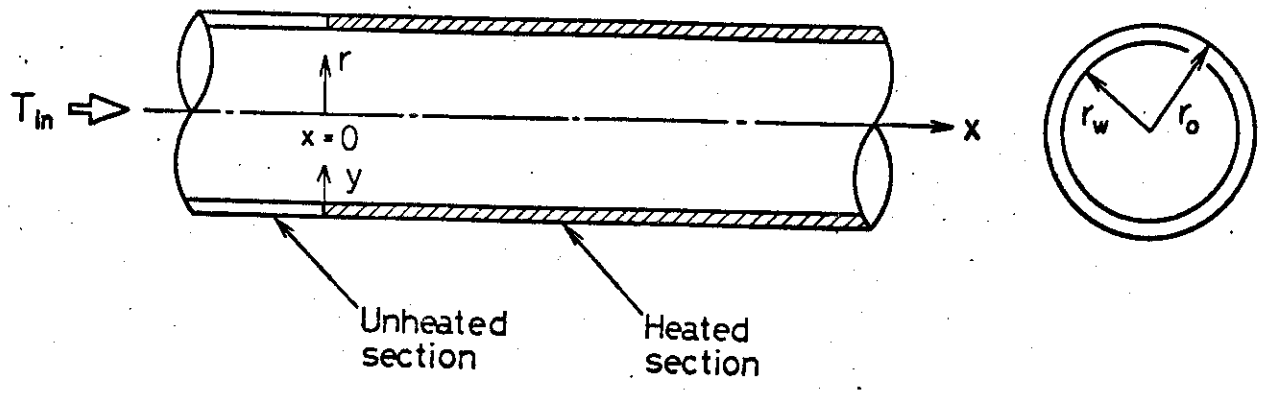

Fig. 1 Co-ordinate system.

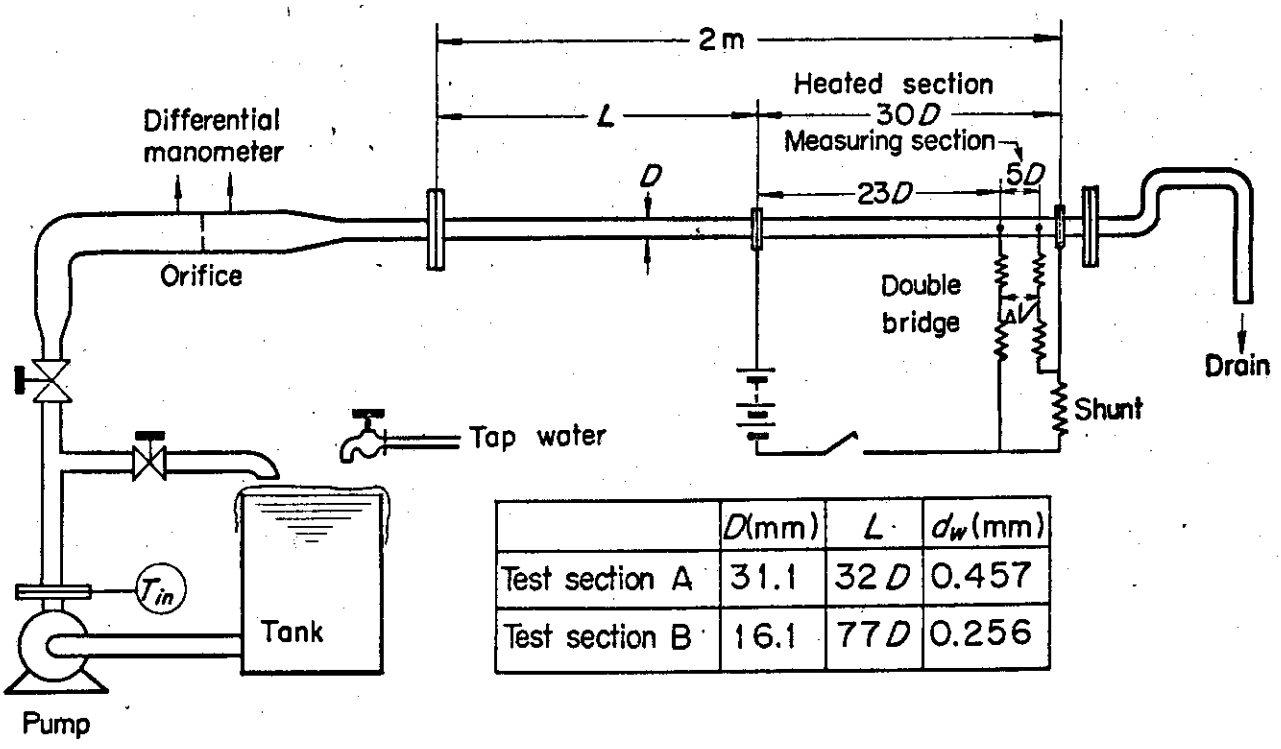

	D(mm)	L	d_w(mm)
Test section A	31.1	32D	0.457
Test section B	16.1	77D	0.256

Fig. 2 Experimental apparatus for power transient.

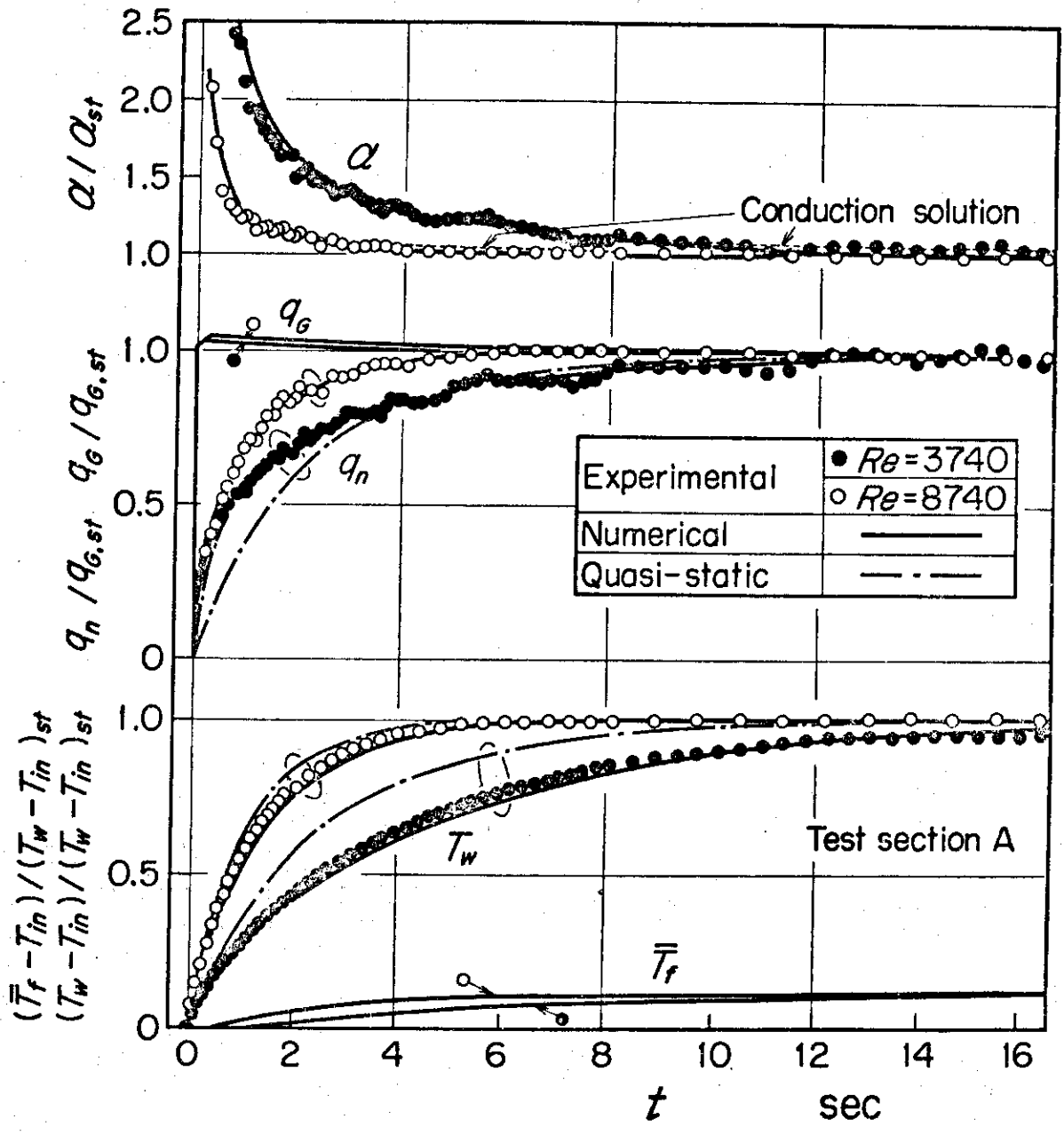

Fig. 3 Experimental and analytical results on power transient.

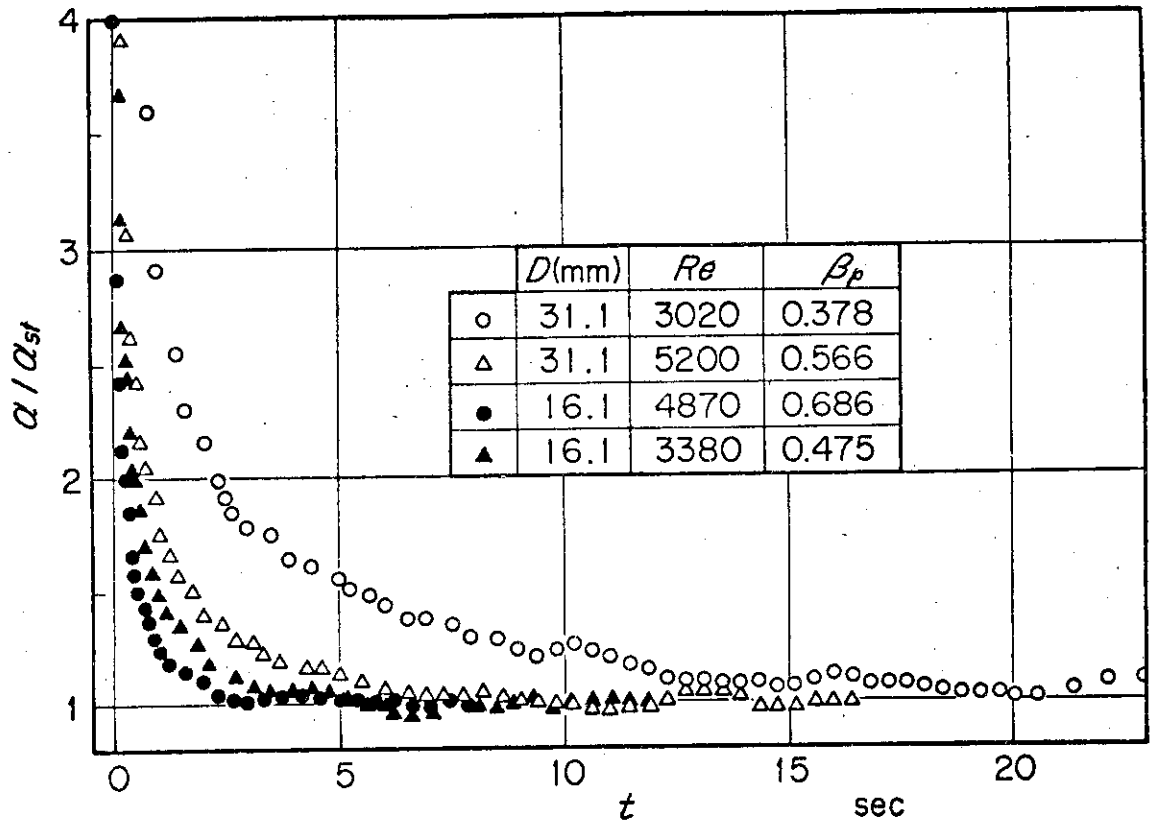

Fig. 4(a) Variation of heat transfer coefficient plotted versus real time in sec.

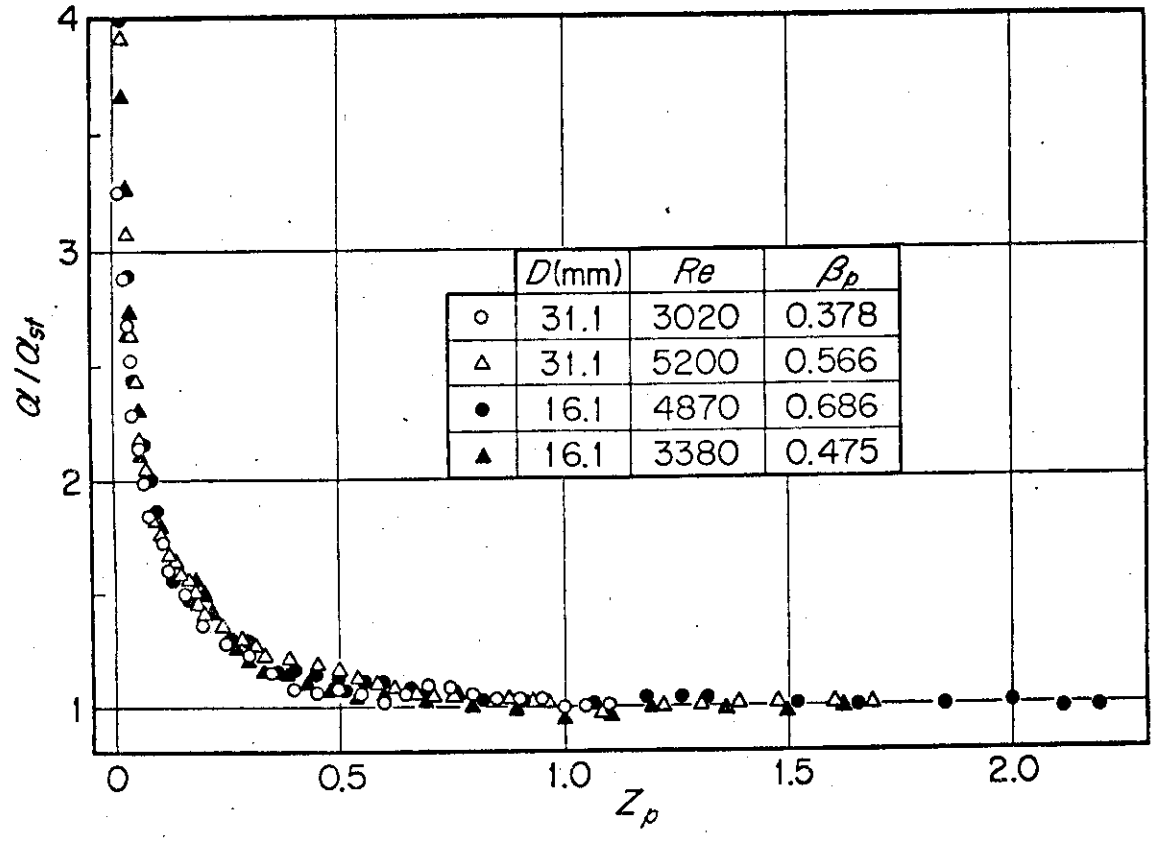

Fig. 4(b) Variation of heat transfer coefficient plotted versus non-dimensional time Z_p.

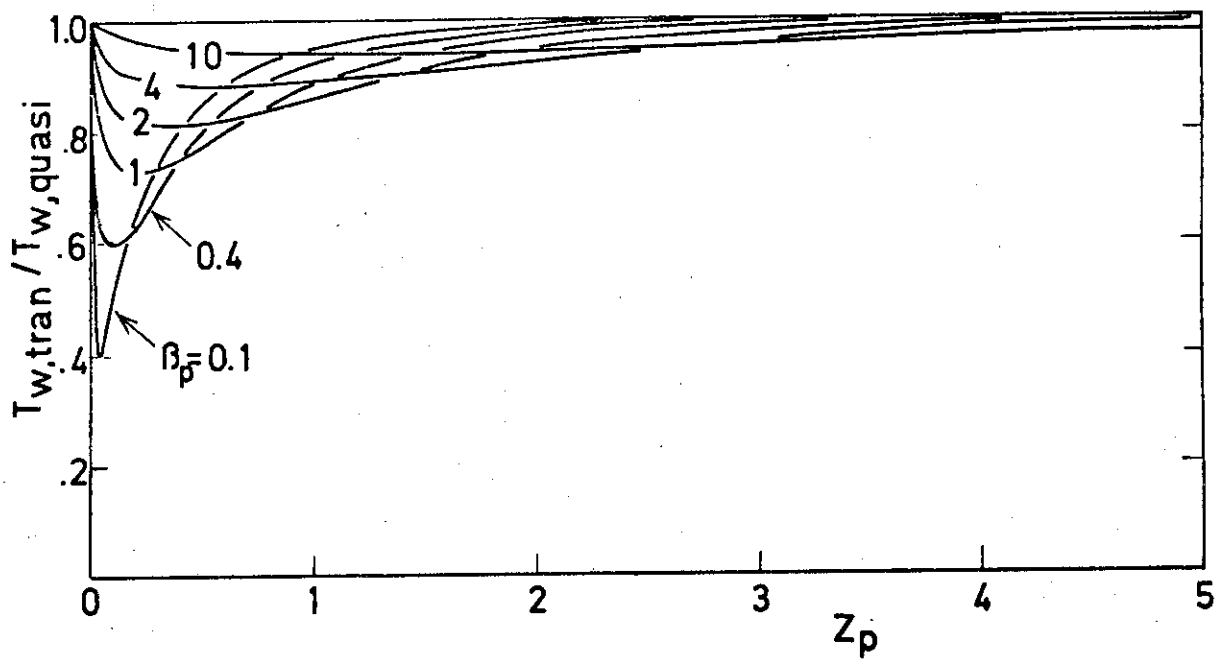

Fig. 5 Error in wall temperature due to the quasi-static assumption (power transient).

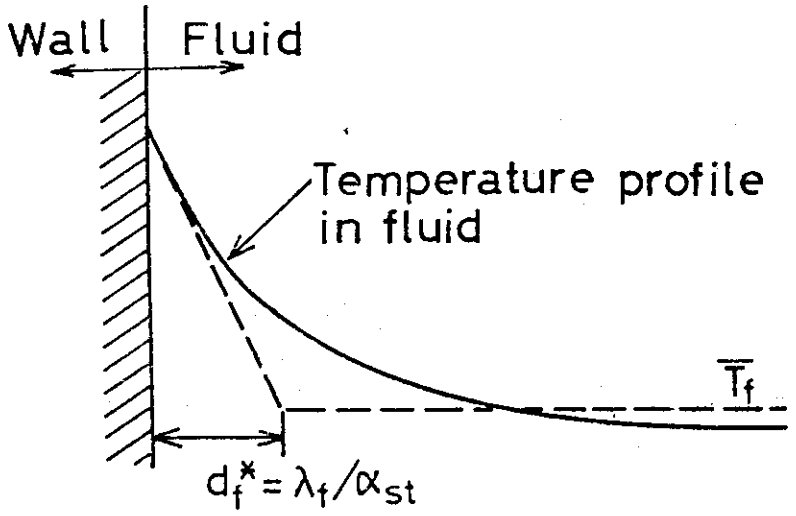

Fig. 6 Equivalent thermal boundary layer thickness.

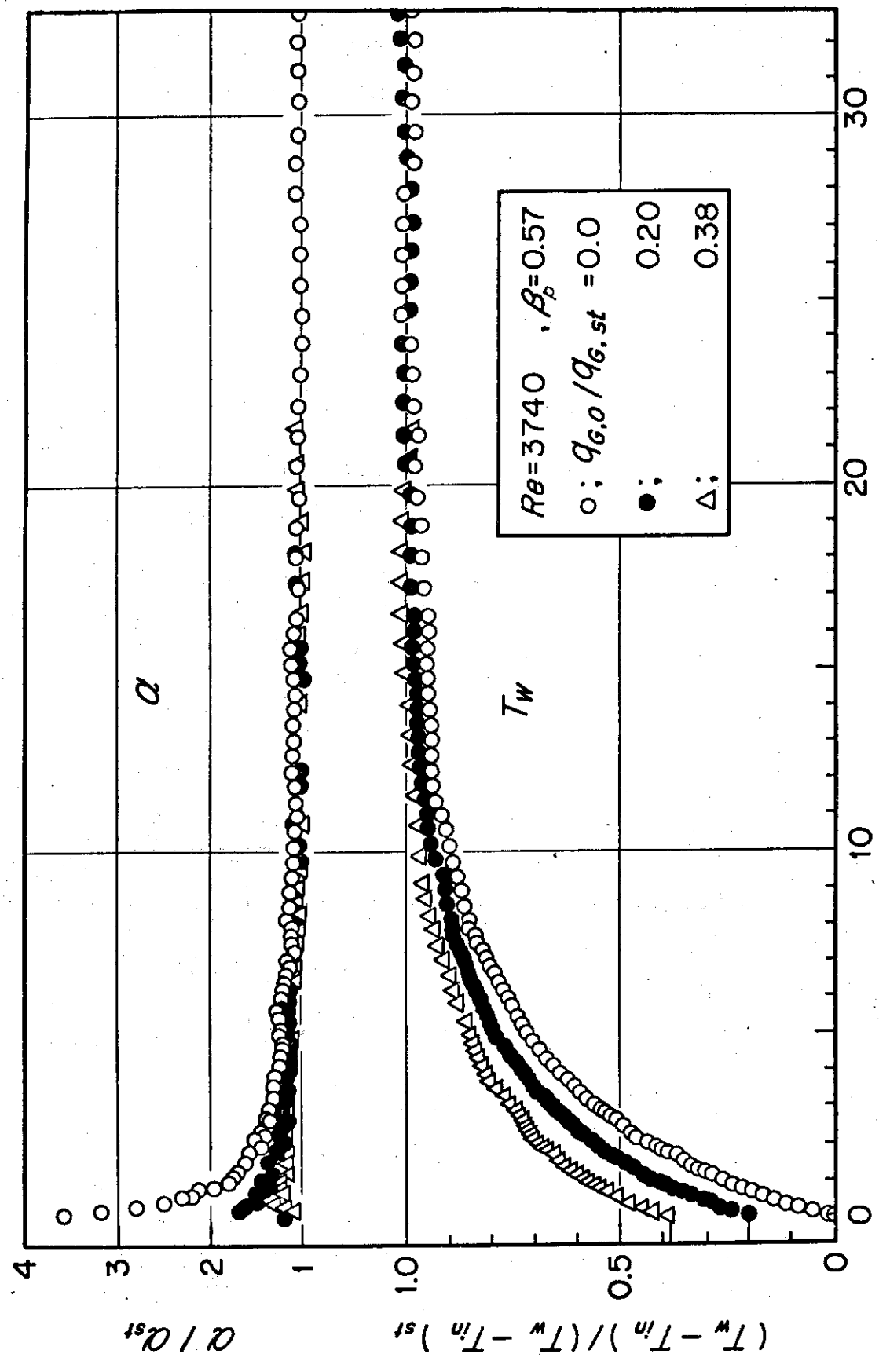

Fig. 7 Effect of initial heat input for power transient.

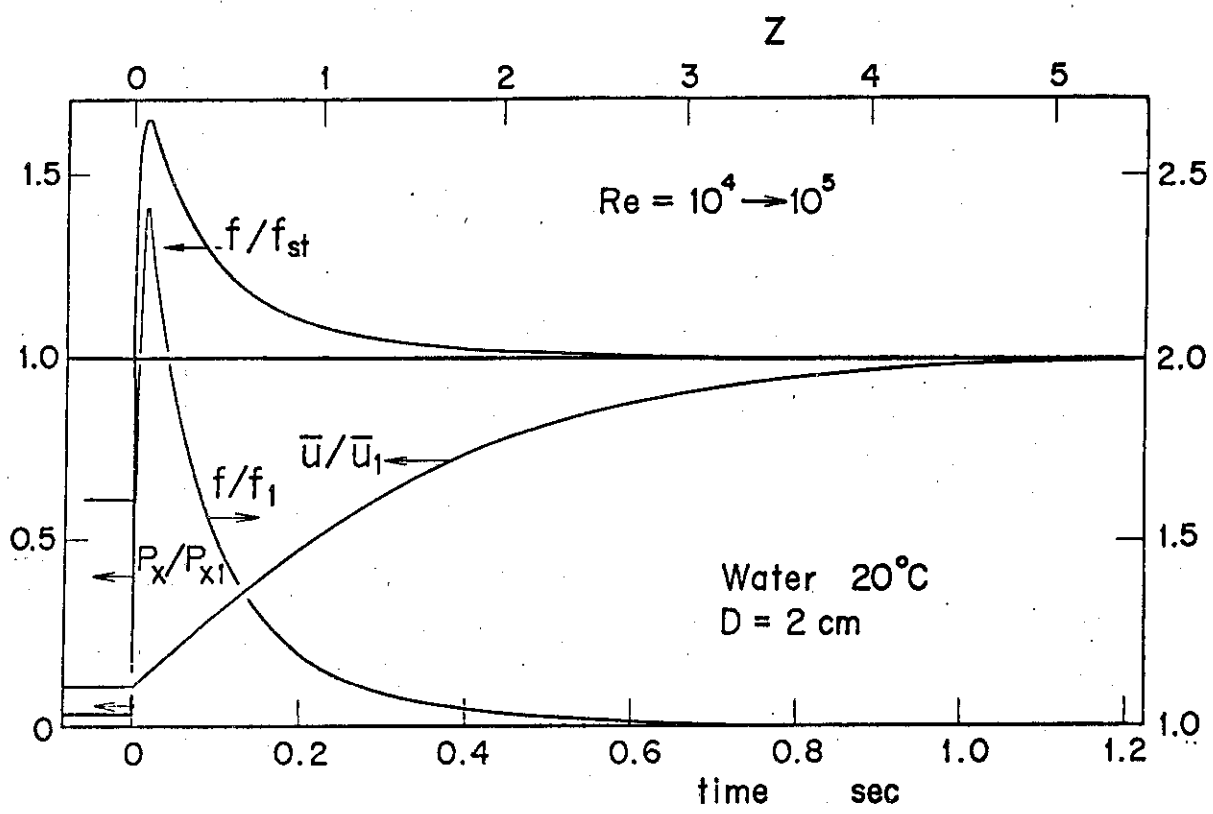

Fig. 8 Numerical results on accelerated flow.

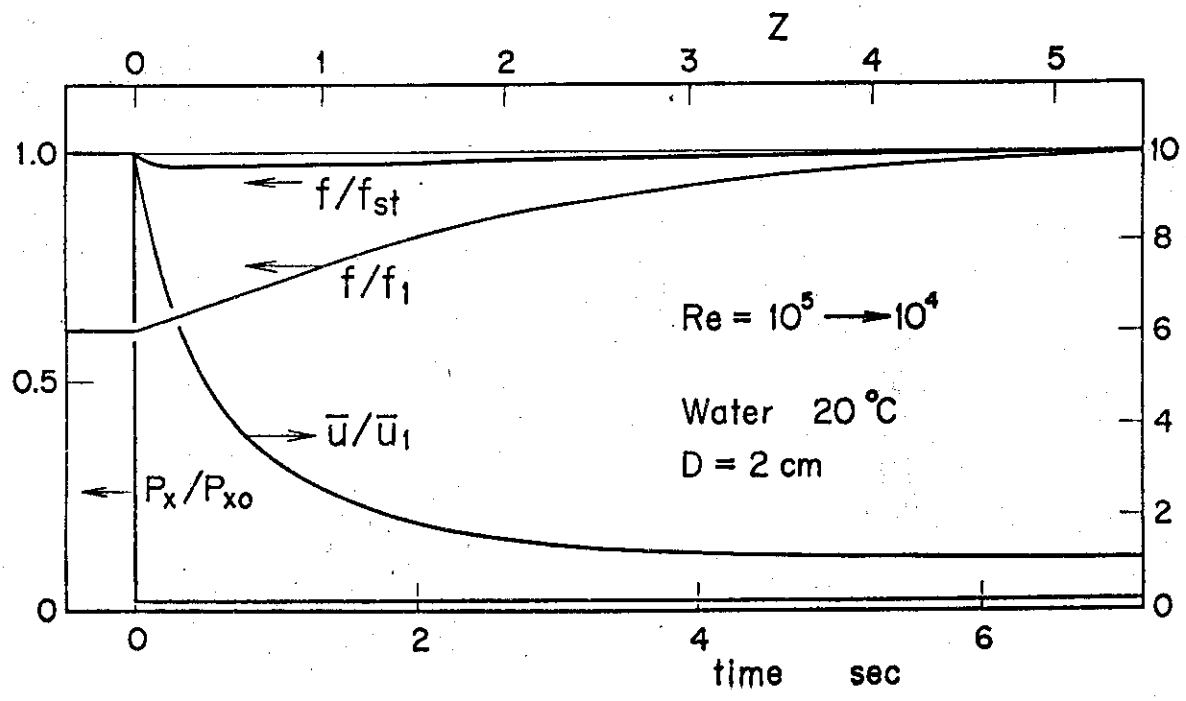

Fig. 9 Numerical results on decelerated flow.

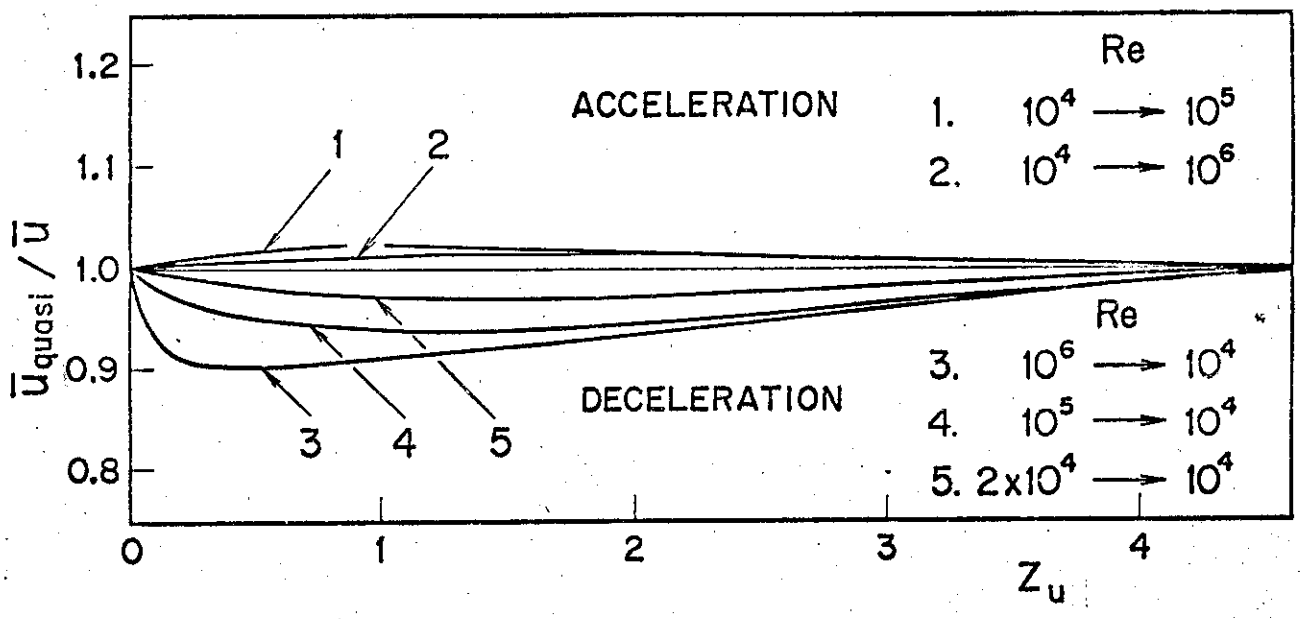

Fig. 10 Error in velocity due to the quasi-static assumption (flow transient).

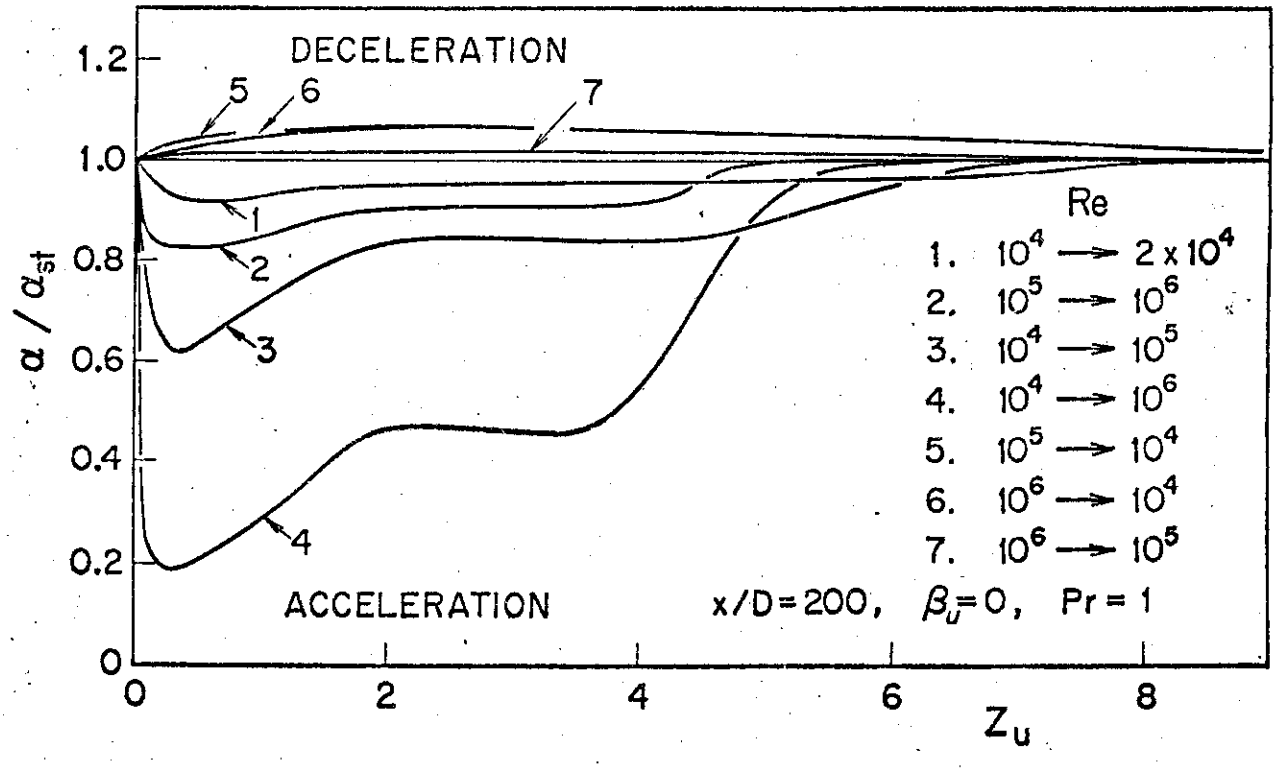

Fig. 11 Variation of α/α_{st} in flow transient.

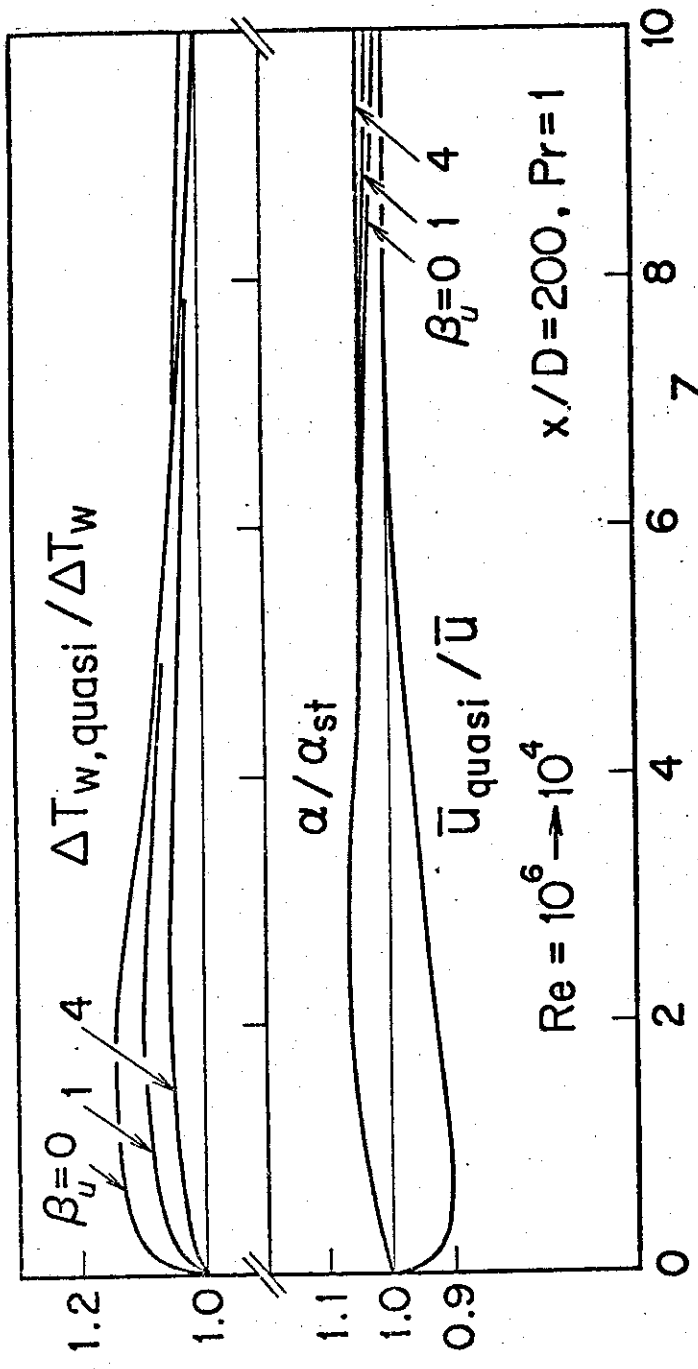

Fig. 12 Error in wall temperature due to the quasi-static assumption for flow deceleration.

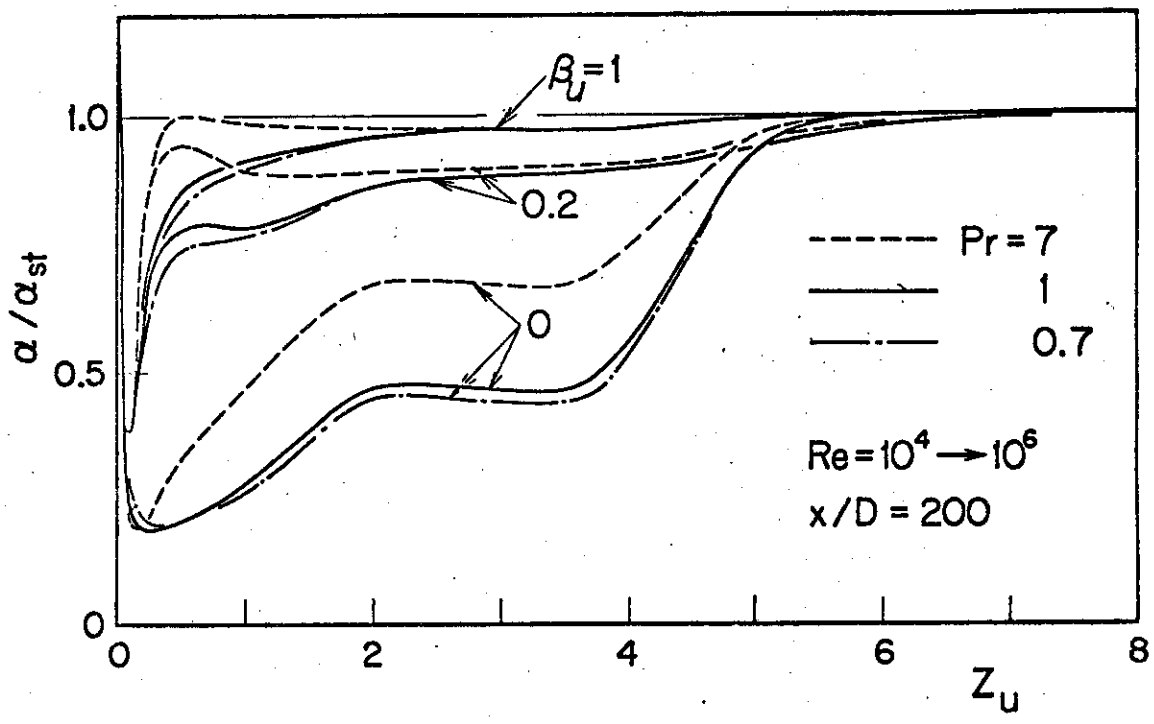

Fig. 13 Effects of Pr and wall heat capacity on α/α_{st} in accelerated flow.

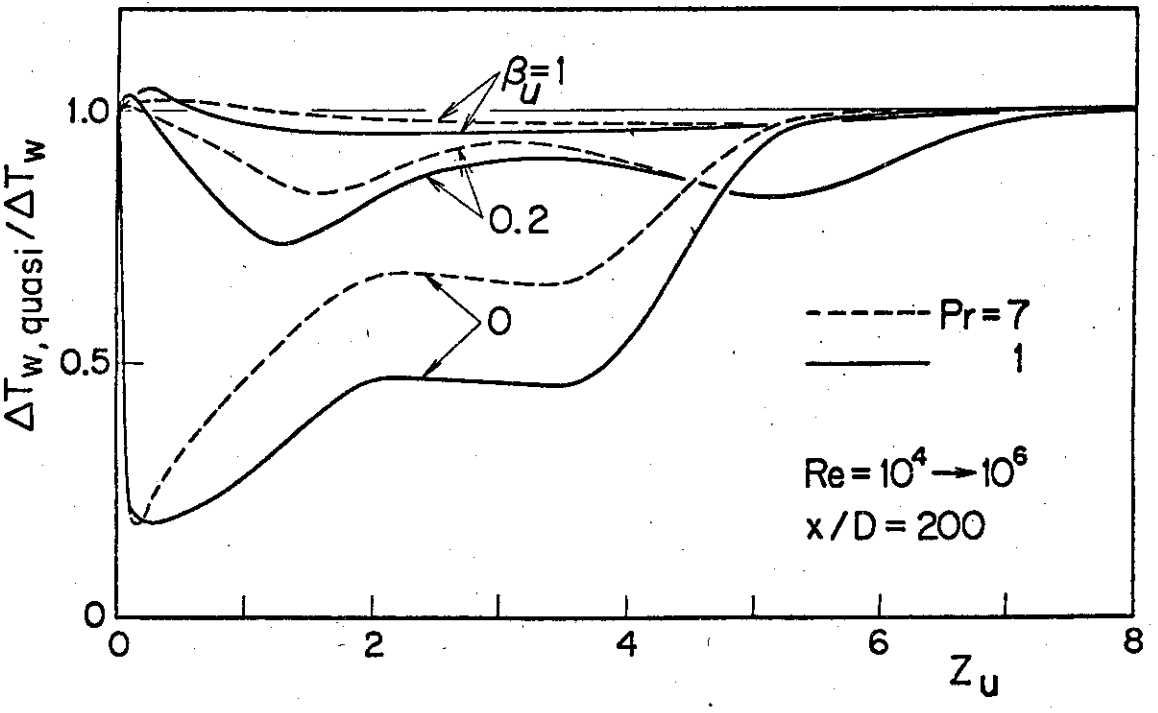

Fig. 14 Error in wall temperature due to the quasi-static assumption for flow acceleration.

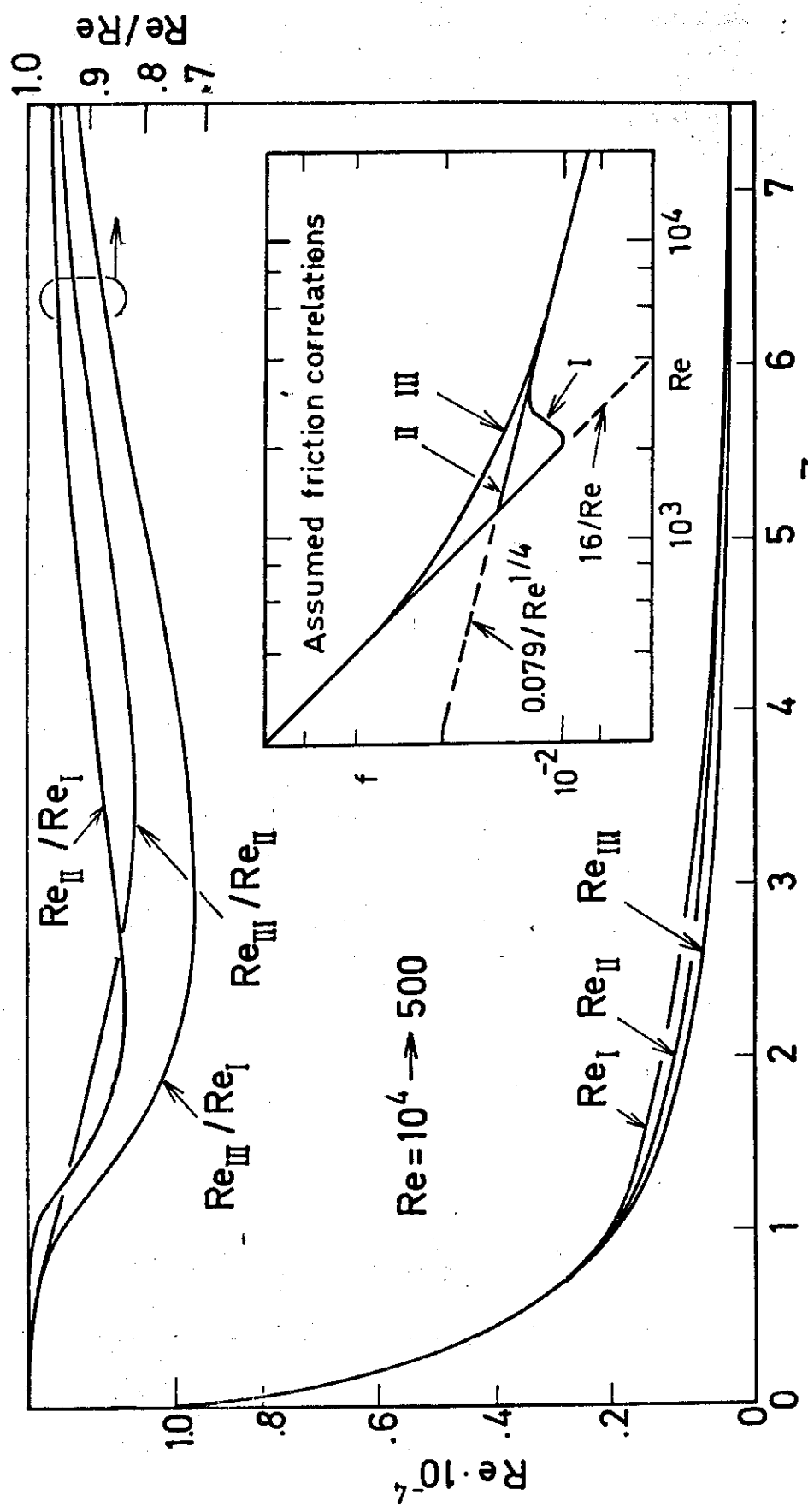

Fig. 15 Flow deceleration calculated with different friction correlations.